Optical Engineering

OpticalEngineering.SPIEDigitalLibrary.org

Influence of stimulated Brillouin scattering on positioning accuracy of long-range dual Mach–Zehnder interferometric vibration sensors

Xiangge He
Shangran Xie
Shan Cao
Fei Liu
Xiaoping Zheng
Min Zhang
Han Yan
Guocai Chen

SPIE.

Xiangge He, Shangran Xie, Shan Cao, Fei Liu, Xiaoping Zheng, Min Zhang, Han Yan, Guocai Chen, "Influence of stimulated Brillouin scattering on positioning accuracy of long-range dual Mach–Zehnder interferometric vibration sensors," *Opt. Eng.* **55**(11), 116111 (2016), doi: 10.1117/1.OE.55.11.116111.

Influence of stimulated Brillouin scattering on positioning accuracy of long-range dual Mach–Zehnder interferometric vibration sensors

Xiangge He,[a] Shangran Xie,[b] Shan Cao,[a] Fei Liu,[a] Xiaoping Zheng,[a] Min Zhang,[c,*] Han Yan,[d] and Guocai Chen[d]
[a]Tsinghua University, Department of Electronic and Engineering, No. 30 Shuangqing Road, Haidian District, Beijing 100084, China
[b]Max Planck Institute for the Science of Light, Staudtstr. 2, Erlangen 91058, Germany
[c]Peking University, Institute of Ocean Research, No. 5 Yiheyuan Road, Haidian District, Beijing 100871, China
[d]China State Shipbuilding Corporation, System Engineering Research Institute, No. 16 Cuiwei Road, Haidian District, Beijing 100036, China

Abstract. The properties of noise induced by stimulated Brillouin scattering (SBS) in long-range interferometers and their influences on the positioning accuracy of dual Mach-Zehnder interferometric (DMZI) vibration sensing systems are studied. The SBS noise is found to be white and incoherent between the two arms of the interferometer in a 1-MHz bandwidth range. Experiments on 25-km long fibers show that the root mean square error (RMSE) of the positioning accuracy is consistent with the additive noise model for the time delay estimation theory. A low-pass filter can be properly designed to suppress the SBS noise and further achieve a maximum RMSE reduction of 6.7 dB. [DOI: 10.1117/1.OE.55.11.116111]

Keywords: distributed fiber vibration sensing; dual Mach–Zehnder interferometer; stimulated Brillouin scattering; time delay estimation.

Paper 161331 received Aug. 25, 2016; accepted for publication Nov. 3, 2016; published online Nov. 23, 2016.

1 Introduction

Dual Mach–Zehnder interferometric (DMZI) vibration sensors can detect acoustic vibrations along the fiber, having the advantages of a long sensing distance, high sensitivity, and the ability of precision positioning. They have been widely applied in many areas, including oil pipeline monitoring, communication optical cable monitoring, and perimeter securities.[1–4] As a phase-modulated sensor, DMZI is very sensitive to external vibration events, while on the other hand it is also fairly easily affected by noise. To realize event positioning, the key function of DMZI, a cross-correlation algorithm is normally used to estimate the time delay between the bidirectional signals traveling along two interferometers caused by the same event. Previously, Quazi etc. developed the estimation model only considering additive noises.[5–7] By considering both additive and multiplicative noises, Xie et al.[8] have proposed the prediction theory on the positioning RMSE for DMZI vibration sensors.

In recent years, ultralong distance vibration sensing has attracted much interest to further extend the applications of DMZI. Tu et al.[9] reported a DMZI system with 160 m positioning precision on a 112-km-long sensing fiber. In this system, four single mode fibers (SMFs) in an optical cable were used. Two of them form the interference arms and others are lead fibers.

In long distance sensing applications, due to the presence of fiber loss, the power injected into the fiber needs to be high enough to get enough signal-to-noise ratio (SNR) on the photodetector, noting the minimum power arriving at the detector as $P_{\min}$. Given the fiber attenuation coefficient α and length L, the minimum power injected into the interference arm can be written as

$$P_{IN\,\min} = P_{\min}\,\exp(2\alpha L)/2. \tag{1}$$

Here the lengths of both sensing and lead fibers in real systems using one optical cable are considered.[9,10] On the other hand, a nonlinear effect (e.g., stimulated Brillouin scattering, SBS) starts to appear when its threshold P_{th} is reached[11]

$$P_{\text{th}} = 21 \cdot \frac{KA_{\text{eff}}}{g_B L_{\text{eff}}} \cdot \frac{\Delta\nu_P + \Delta\nu_B}{\Delta\nu_B}, \tag{2}$$

where K is the polarization factor, A_{eff} is the effective mode area of the fiber, g_B is the Brillouin peak gain coefficient, $L_{\text{eff}} = [1 - \exp(-\alpha L)]/\alpha$ is the effective length, and $\Delta\nu_p$ and $\Delta\nu_B$ are the linewidth of the pump light and Stokes light, respectively.

For standard SMF and typical photodetectors, $A_{\text{eff}} = 80\ \mu\text{m}^2$, $g_B = 5 \times 10^{-11}$ m/W, $\alpha = 0.21$ dB/km, and $P_{\min}$ is typically 5 μW. Under such conditions, when P_{th} is reached, the sensing fiber length L is ~70 km. This means that to achieve longer distance fiber sensing, the noises contributed from a nonlinear effect should be considered. Since the interference signals in the DMZI system are bidirectional, the backscattering of a clockwise signal will bring noise into the counterclockwise signal and vice versa. Therefore, to achieve long-range vibration sensing, SBS noise could be a critical limiting factor, the contribution of which on the positioning accuracy of a DMZI system has so far not been studied.

In this paper, the properties of SBS noise in an interference system are experimentally measured. The influence of SBS noise on the positioning accuracy of the DMZI vibration sensor is further studied. It is found that SBS noise is white and incoherent in the 1-MHz bandwidth range and can be treated as an additive noise term in the positioning accuracy estimation model. We also show that a low-pass

*Address all correspondence to: Min Zhang, E-mail: 1606871001@pku.edu.cn

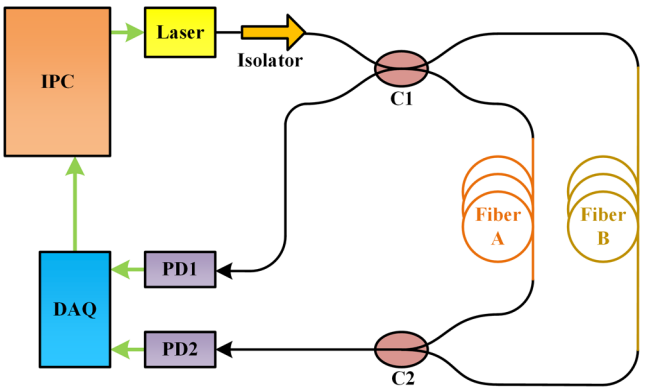

Fig. 1 Experimental setup to study the properties of SBS noise in interferometer.

filter with a proper design can efficiently suppress SBS noise achieving a maximum positioning root mean square error (RMSE) reduction of 6.7 dB.

2 SBS Noise in Interferometric System

Figure 1 shows the experimental setup we used to investigate the properties of SBS noise in interference signals. A narrow linewidth laser beam at 1550-nm wavelength (NKT Koheras BasiK E15) was injected into the interferometer after going through an isolator to suppress backreflection. Note that even though a broadband (or phase-scrambled) laser source can be used to significantly increase the SBS threshold, a narrow linewidth laser is used here to guarantee a high enough interference visibility and thus the SNR in the detection end, especially when the exact matching of the lengths of the two arms are difficult in practice. The MZI was formed by 50:50 fiber couplers C1 and C2 and two spools of 25-km G652D SMFs (A and B). Photodetectors PD1 and PD2 were used to collect the backscattered and transmitted signals, respectively. Data were collected via a high-speed data acquisition card and then were further processed in an industrial personal computer (IPC). The IPC can also adjust the output power of the laser.

In the experiment, the power launched into fibers A and B was varied from 3.6 to 8.4 mW with a 0.4 mW step. First, just fiber A or B was connected and the transmitted and backscattered signals of it were measured (labeled as single-arm). Then both fibers A and B were connected and their interference signals were measured (labeled as dual-arm). Since the frequency of the intrusion event is often lower than tens of kHz in practical applications,[9] the bandwidth we measured is 1 MHz.

Figure 2 compares the typical time-domain and frequency-domain transmitted and backscattered signals for single-arm and dual-arm cases, at an input power of 6.8 mW. For single-arm, the energy of the transmitted signal [Figs. 2(a) and 2(b)] is mainly distributed below 100 kHz while the backscattered signal [Figs. 2(e) and 2(f)] shows a stochastic fluctuation both in the time domain and frequency domain. The result agrees with Horowitz's research,[12] who found that the transmitted noise bandwidth of Brillouin scattering was ~90 kHz while the backward noise bandwidth was about tens of MHz. In addition, the intensity of the backscattered signal is two orders of magnitude higher than that of the transmitted signal, as the input power is well above the SBS threshold. For dual-arm, the transmitted signal shows interference fringes in the time-domain [Fig. 2(c)] and its energy is mainly distributed below 200 Hz, primarily due to the contribution from the environmental noises. But the backscattered signal [Figs. 2(g)–2(j)] shows a stochastic fluctuation in the time domain and a fairly uniform energy distribution in the frequency domain, in sharp contrast to the transmitted signal.

The statistical properties of the temporal behavior of the Brillouin Stokes signal have been investigated by Gaeta and Boyd,[13] in which large stochastic fluctuations were resolved for SMF. In our experiment, we show that the stochastic fluctuation not only exists in a single piece of fiber, but also for the dual-arm interferometers, as plotted in Fig. 2(g). In Gaeta's theory, the SBS medium behaves as a linear amplifier for the thermal noise that initiates the SBS process. Thermal noise can be assumed as a Gaussian random process, and the spectrum of the amplified Stokes field is also predicted to be Gaussian. As a result, the Stokes signals

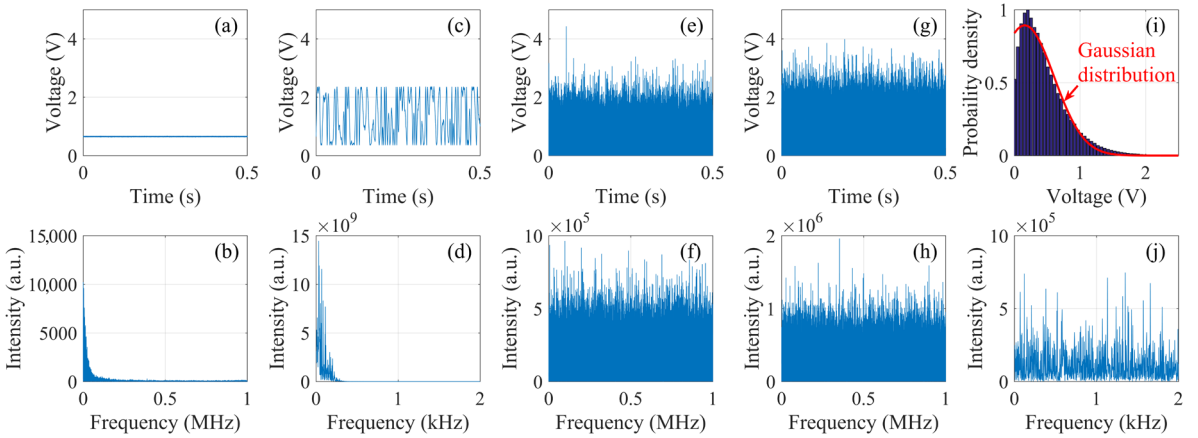

Fig. 2 Time-domain transmitted signals for (a) single-arm, (c) dual-arm, with the corresponding power spectrum shown in (b) and (d). Time-domain backscattered signals for (e) single-arm, (g) dual-arm, with the corresponding power spectrum shown in (f) and (h). (i) plots the histogram of (g) with the red line fitted Gaussian distribution. (j) is the same as (h) with frequency range to 2 kHz, showing the detail of low frequency.

of the two arms of the interferometer will not interfere with each other, explaining the observed stochastic fluctuation and the Gaussian distribution of the time domain interference signal [see Fig. 2(i)]. The SBS process, therefore, introduces white noise into the system without interference noise.

To further validate that the SBS noise does not introduce interference, the average intensities of the transmitted and backscattered signals were measured at different input powers, as plotted in Fig. 3. The red-triangles, blue-triangles, and black-asterisks represent the cases of single fibers A, B, and interference signals, respectively. The pink circles represent the sum of single fibers A and B (labeled as sum AB). As seen in the figures, SBS starts to occur when the input power reaches 4.8 mW. In the transmitted case, the average intensities of sum AB are different from that of the dual-arm interference signals, indicating the coherent property of the transmission. For backscattered signals, due to the lack of interference, sum AB are the exactly the same as that of the dual-arm configuration. Note that in this measurement, an average time of 0.5 s was applied to suppress the random noise while at the same time partially retaining the coherence information of the signal.

3 Influence of SBS Noise on the Positioning Accuracy of DMZI

Figure 4 sketches the experimental setup to study the positioning accuracy of DMZI with the presence of SBS noise. Couplers 2 and 3 along with fibers A and B form the DMZI structure. Both fibers A and B are 25 km long. A polarization controller was used to align the polarization state in fibers A and B.[9] Vibration events were generated by a piezoelectric ceramic transducer (PZT) near one end of fiber B. The PZT was driven by a 1-kHz sinusoidal wave generated by a signal generator. The rest of the system is the same as that illustrated in Fig. 1.

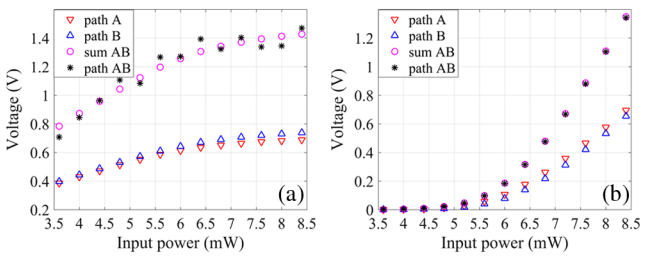

Fig. 3 The average intensities of (a) transmitted and (b) backscattered signals.

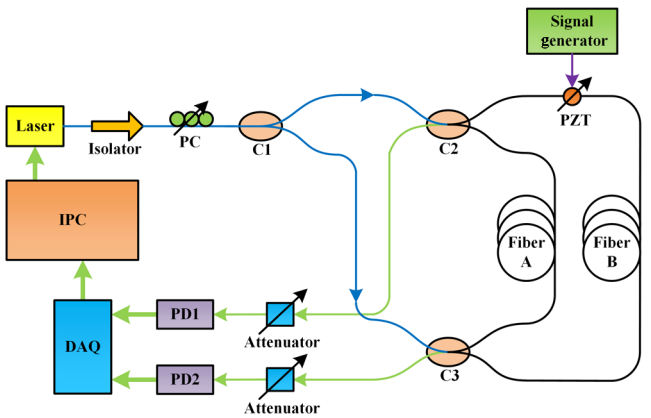

Fig. 4 Experimental setup to measure the positioning accuracy of DMZI.

In this experiment, the input power was varied from 3.6 to 8.0 mW with 0.4 mW as the step. For each input power, 250 experiments were conducted to obtain the positioning RMSE. Crosscorrelation algorithm was applied to estimate the time delay $\widehat{D}$ with the unit of sampling point ($\Delta t = \widehat{D}/f_s$, where Δt is the time delay in seconds and f_s is the sampling frequency). The RMSE of $\widehat{D}$ can be expressed as

$$\mathrm{RMSE}_{\mathrm{pt}} = \sqrt{\frac{1}{250}\sum_{i=1}^{250}(\widehat{D}_i - D)^2}, \tag{3}$$

where D is the real value of the time delay, $\widehat{D}_i$ is the estimated value for trial number i, and $\mathrm{RMSE}_{\mathrm{pt}}$ is the RMSE with the unit of sampling point. Equation (4) was used to convert from $\mathrm{RMSE}_{\mathrm{pt}}$ to RMSE in dB

$$\mathrm{RMSE(dB)} = 10\log_{10}(\mathrm{RMSE}_{\mathrm{pt}}). \tag{4}$$

Figure 5 shows the experimental results. The blue-triangles and red-dots represent the SNR and RMSE (both in dB) versus the input power, respectively. Here the SNR is defined as $\mathrm{SNR} = 10 \times \log_{10}(P_{\mathrm{signal}}/P_{\mathrm{noise}})$ where P_{signal} and P_{noise} is the power of the 1-kHz sinusoidal signal (calculated by integrating the power spectral density from 500 to 1500 Hz) and the background noise, respectively. It can be clearly seen that above the SBS threshold (4.8-mW input power), SNR starts to decrease and RMSE starts to increase dramatically with input power, while below the SBS threshold both SNR and RMSE barely change with input power.

The model developed by Quazi and Ianniello[5,6] can be used to predict the error of time delay estimation (TDE) when considering the additive noises.[8,10] Figure 6(a) plots the simulation results of σ_{CRLB} and σ_{CPE} when $T = 0.5$ s and $B = 3$ kHz (the bandwidth B is obtained by Welch power spectrum estimation method[14] in the experiment), where σ_{CRLB} is the standard deviation of the Cramer–Rao lower bound (CRLB) for TDE, σ_{CPE} is the standard deviation of the correlator performance estimate (CPE) for TDE, T is the observation window, and B is the bandwidth. CPE is more accurate for the crosscorrelation algorithm in the

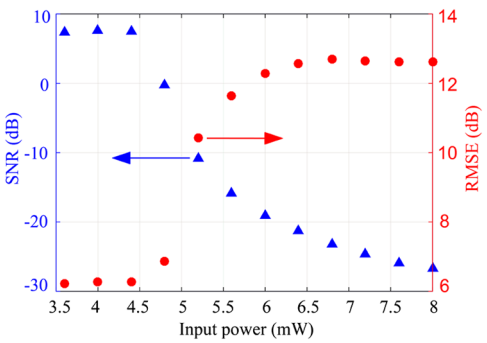

Fig. 5 The measured SNR (left blue Y axis) and RMSE (right red Y axis) at different input powers.

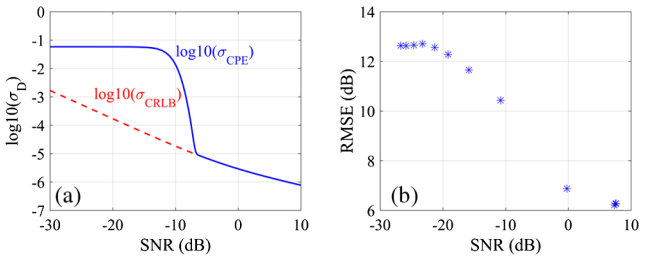

Fig. 6 (a) Simulated and (b) measured RMSE versus SNR.

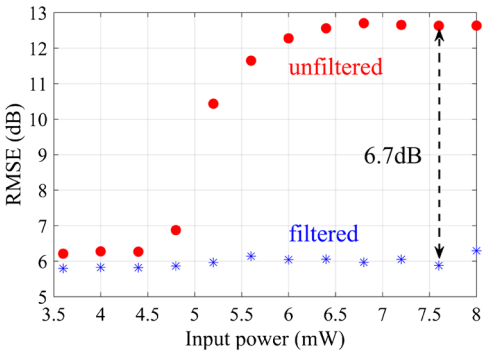

Fig. 7 Comparison of positioning RMSE between unfiltered and filtered interference signals at different input powers.

presence of large estimation errors or anomalous estimates.[7] As can be seen in Fig. 6(a), when SNR is lower than about −6 dB, the predicted RMSE starts to increase rapidly, while when SNR is lower than −15 dB, the RMSE remains almost unchanged. Figure 6(b) shows the measured RMSE versus SNR in our experiment. It can be seen that from 0 to −23 dB, RMSE increases rapidly with the decrease of SNR, and when the SNR is lower than −23 dB the RMSE remains unchanged, which agrees well with the theoretical trend predicted in Fig. 6(a), which confirms the additive and incoherence properties of SBS noise. The experimentally measured RMSEs are larger than theoretical prediction. We attribute this difference to the residue polarization-induced fading effect caused by environmental noises accumulated along the entire bare optical fiber used in the experiment.[2]

Finally, we apply a low pass digital filter to suppress the influence of SBS noise. A Chebyshev type I digital filter, with a cut-off frequency of 1.5 kHz, was inserted right before the crosscorrelation calculation in the algorithm, to filter out the noises of the bidirection signals. The applied filter can maintain the signal below 1 kHz and at the same time remove the most high frequency SBS noise. Figure 7 compares the filtered (blue) and unfiltered (red) results of positioning RMSE versus input power. It can be seen that a maximum reduction of about 6.7 dB can be achieved by using the low-pass filter. The filtered curve in Fig. 7 also shows that the positioning RMSE barely changes before and after SBS occurs (which is not the case for the unfiltered case), confirming the efficient suppression of SBS noise by the filter. A ∼6 dB of RMSE in the filtered case corresponds to ∼200-m positioning error, which is mainly limited by the residual environmental noises mentioned in Sec. 2.

4 Conclusion

The influences of SBS noise in DMZI vibration sensing systems are reported. Through detailed analysis of time-domain and frequency-domain properties, we show that SBS noise is a white noise and does not introduce interference between the two arms of the interferometer in a 1-MHz bandwidth range. Vibration positioning experiments on 25-km long bare SMF are conducted with the presence of SBS noise. The additive property of the SBS noise is supported by the agreement in trend of positioning RMSE versus SNR with the theoretical model. We also show that a maximum value of 6.7-dB RMSE reduction can be achieved by applying a low-pass filter with proper parameters. The results presented here can be further applied to any other fiber interferometric systems.

References

1. A. Mendez, T. F. Morse, and F. Mendez, "Applications of embedded optical fiber sensors in reinforced concrete buildings and structures," *Proc. SPIE* **1170**, 60–69 (1990).
2. J. Wu, "Study on locating technology of distributed optic-fiber sensing system based on interfering principle for long-distance pipelines sabotage acts," M.S. Thesis, Department Opto-Electronics Engineering, Chongqing University, Chongqing, China (2007).
3. L. Sheng et al., "Fiber-optic intrinsic distributed acoustic emission sensor for large structure health monitoring," *Opt. Lett.* **34**(12), 1858–1860 (2009).
4. X. Li, "The intrusion signal recognition of perimeter security for distributed the fiber-optic senor," M.S. Thesis, Department of Information Engineering, Xiangtan University, Hunan, China (2013).
5. H. Quazi, "An overview on the time delay estimate in active and passive systems for target localization," *IEEE Trans. Acoust. Speech Signal Process.* **29**(3), 527–533 (1981).
6. J. P. Ianniello, "Time delay estimation via cross-correlation in the presence of large estimation errors," *IEEE Trans. Acoust. Speech Signal Process.* **30**(6), 998–1003 (1982).
7. K. Scarbrough, R. J. Tremblay, and G. C. Carter, "Performance predictions for coherent and incoherent processing techniques of time delay estimation," *IEEE Trans. Acoust. Speech Signal Process.* **31**(5), 1191–1196 (1983).
8. S. Xie et al., "Positioning error prediction theory for dual Mach-Zehnder interferometric vibration sensor," *J. Lightwave Technol.* **29**(3), 362–368 (2011).
9. D. Tu et al., "Ultra long distance distributed fiber-optic system for intrusion detection," *Proc. SPIE* **8561**, 85611W (2012).
10. S. Xie et al., "Positioning error reduction technique using spectrum reshaping for distributed fiber interferometric vibration sensor," *J. Lightwave Technol.* **30**(22), 3520–3524 (2012).
11. M. W. Zmuda, "Stimulated Brillouin scattering effects and suppression techniques in high power fiber amplifiers," Ph.D. dissertation, Department Optical Science Engineering, New Mexico University, Albuquerque (2009).
12. M. Horowitz et al., "Broad-band transmitted intensity noise induced by Stokes and anti-Stokes Brillouin scattering in single-mode fibers," *IEEE Photonics Technol. Lett.* **9**(1), 124–126 (1997).
13. L. Gaeta and R. W. Boyd, "Stochastic dynamics of stimulated Brillouin scattering in an optical fiber," *Phys. Rev. A* **44**(5), 3205–3209 (1991).
14. A. V. Oppenheim and R. W. Schafer, *Digital Signal Process*, Prentice-Hall, New Jersey (1975).

Xiangge He received his BE degree in optoelectronic science and engineering from Huazhong University of Science and Technology, Wuhan, China, in 2012. He is working toward his DE degree at Tsinghua University. His research interests include distributed optical fiber sensors.

Fei Liu received his BSc degree in the College of Precision Instrument and Opto-electronics Engineering from Tianjin University, China, in 2012. Currently, he is working toward the PhD from the Department of Electronic Engineering in Tsinghua University.

Biographies for the other authors are not available.